ECASIA SPECIAL ISSUE PAPER

WILEY SURFACE and INTERFACE ANALYSIS

Development and characterization of hydrophobic anodized aluminum layer to act as a long-lasting protective film in corrosion

R. Jaimes-Ramírez[1] | A. Covelo[1] | S. E. Rodil[2] | P. Corona-Lira[1] | A. C. Ramírez-Reivich[1] | M. Hernández[1]

[1] División de Ingeniería Mecánica e Industrial (DIMEI), CENISA, Facultad de Ingeniería, UNAM, 04510 Mexico City, Mexico

[2] Instituto de Investigaciones en Materiales, UNAM, 04510 Mexico City, Mexico

Correspondence
Miguel Hernández, División de Ingeniería Mecánica e Industrial (DIMEI), CENISA, Facultad de Ingeniería, UNAM, 04510, Mexico City, Mexico.
Email: mahdz2010@comunidad.unam.mx

This work focuses on the development of a novel hydrophobic process for anodized aluminum AA2024-T3 which consists of a combination of corrosion inhibitors: sodium metavanadate with a γ-irradiated fluoropolymer. The anodizing films, formed in sulfuric acid media, were sealed by using different aqueous solutions such as boiling water, potassium dichromate, and cerium nitrate. The corrosion resistance results obtained by electrochemical impedance spectroscopy (EIS) showed that samples sealed with $Ce(NO_3)_3$ had a higher average value of total impedance of 10^{11} Ω cm^2 obtained at low frequencies in 0.1 M NaCl solution. Water contact angle measurements revealed best results at 128.8°. X-ray photoelectron microscopy in conjunction with scanning electron microscopy indicated the formation of a layer of fluoro compound above the anodized aluminum. X-ray diffraction, infrared spectroscopy, and differential scanning calorimetry demonstrated thermal modifications of the γ-irradiated fluoropolymer.

KEYWORDS

γ-irradiation, anodized aluminum, fluoropolymer, hydrophobicity

1 | INTRODUCTION

A well-known electrochemical process that is used to increase the corrosion resistance and the adhesion properties of aluminum surfaces is the electrochemical anodizing process involving an electrochemical reaction in acidic electrolytes which increases the thickness of the aluminum oxide layer. Sulfuric acid anodization is extensively used to provide corrosion resistance, wear resistance, and adhesion of polymer coatings with good surface stability.[1]

Anodized aluminum had been studied using corrosion inhibitors such as azoles and tetrazines which have a positive effect on aluminum protection[2]; molybdate compounds influence the corrosion resistance and the anodic film growth, while vanadate compounds give homogeneity within the anodized aluminum layer.[3] Vanadate has demonstrated good corrosion inhibition on aluminum alloys.

To improve corrosion and wear resistance on anodized aluminum, the sealing process after anodizing is necessary given that the oxide pores generated by anodizing that can still absorb aggressive species of the media. Sealing methods block anodic pores to generate a surface with a high resistance to pitting attack.

In addition, a hydrophobic feature for water repellency is needed as a physical barrier to avoid the interaction of destructive species with the metallic interface. Fluorocarbons and silicones are materials with low surface energy used for their hydrophobic properties. To improve the performance of fluoro groups, gamma irradiation is applied to polymers to modify their physical properties and their chemical structure. The irradiation of polymeric materials with gamma rays leads to the formation of very reactive intermediates which result in rearrangements and/or formation of new bonds.[4]

In this study, we developed a multilayer system of corrosion protection of aluminum by using the technique of electrochemical anodization with the incorporation of a γ-irradiated fluoropolymer. The aim is to produce a hydrophobic surface without affecting mechanical and thermal properties of aluminum. This multilayer system showed notable improvement of the corrosion resistance with good electrochemical stability in time.

2 | EXPERIMENTAL

Aluminum AA2024-T3 samples (Si 0.5%, Fe 0.5%, Cu 0.8%-4.9%, Mg 1.2%-1.8%, Mn 0.3%-0.9%, Cr 0.1%, Zn 0.25%, Ti 0.15%, other 0.15%) with dimensions of 2.5 × 3.0 cm were grounded with silicon carbide paper grid (220 to 1000). The aluminum surface was cleaned

in 10% of NaOH at 40°C for 50 seconds, rinsed with distilled water, and dried in a hot stream. Afterwards, the substrate was immersed in 50% HNO_3 at room temperature for 90 seconds. These reagents were purchased from Chemical Reagents Meyer and used as received.

A 2-electrode cell was required for aluminum anodization, which consisted of a working electrode (aluminum substrate) and Pt electrode as a counter electrode which both connected to a DC power supply GPS-3030D. The anodizing process was conducted at room temperature in $H_2SO_4/NaVO_3$ (Sigma-Aldrich) solution for 60 minutes at 1.5 A dm^{-2}.[1] Subsequently, the incorporation of γ-irradiated fluoropolymer into the anodized aluminum surface was conducted by chronoamperometry at 0.23 μA dm^{-2} for 60 minutes.

The fluoropolymer was a fluorosilane emulsion manufactured by Chemguard, Inc. and was gamma irradiated using a γ-source (Gammabeam 651PT, MDS Nordion) in air and in vacuum at room temperature at 500 kGy. The anodizing films with the γ-irradiated fluoropolymer were sealed either with boiling water, potassium dichromate[5] from J.T. Baker, or cerium nitrate[6] from Sigma-Aldrich.

The corrosion behavior of anodized aluminum was conducted by EIS (Autolab Potentiostat PGSTAT204 from 1×10^5 to 0.1 Hz with 10 points/decade). A 3-electrode cell was used for this purpose which consisted of the anodized aluminum as a working electrode, a graphite sheet as a counter electrode and a saturated calomel electrode as a reference electrode. The substrates were immersed in a saline solution of NaCl (0.1 M).

The hydrophobic properties of the anodized film/γ-irradiated fluoropolymer were determined using a water contact angle technique with a Drop Shape Analyzer, Krüss DSA100 at room temperature. The chemical composition was determined by the X-ray photoelectron spectroscopy, using a Physical Electronics equipped with a scanning XPS microprobe PHI 5000 VersaProbe II detector. The measurements were done under ultrahigh vacuum of 4×10^{-8} Pa, and the X-ray source was of Al Kα (hv = 1486.6 eV). The survey scans were recorded using a pass energy of 117.4 eV and a 0.05 energy step. The energy scale was corrected using the scan spectra before surface cleaning using the position of the C1s peak (284.8 eV). Then, survey scans were sequentially recorded after cleaning with Ar^+ ions using different conditions of bombardment to evaluate the in-depth composition. Surface characterization was conducted with SEM equipment JEOL JSM-7600F. X-ray analyses were carried out with a Brucker D8 Advance equipment with monochromatized Cu, Kα of 1.5404 Å, from 2° up to 80°. Infrared analysis was performed with a PerkinElmer Paragon 500 FTIR-ATR in the wavenumber range of 4000 to 650 cm^{-1}. Finally, thermogram analysis using differential scanning calorimetry was conducted with a TA Instrument DSC 2010 at a heating velocity of 10°C min^{-1} with an argon stream at 80 mL min^{-1}.

3 | RESULTS AND DISCUSSION

The SEM and contact angle images are presented in Figure 1. The thickness of hydrophobic/anodized film plays an important role as can be seen in Table 1. Multiple measurements were carried out to estimate the thickness of the hydrophobic/anodized films to reduce the uncertainty values. Figure 1A shows a few cracks on the anodized layer because of using boiling water. Dichromate sealing (Figure 1B) shows a better anodized layer with a defective fluoropolymer film that could affect the corrosion resistance in saline media. On the other
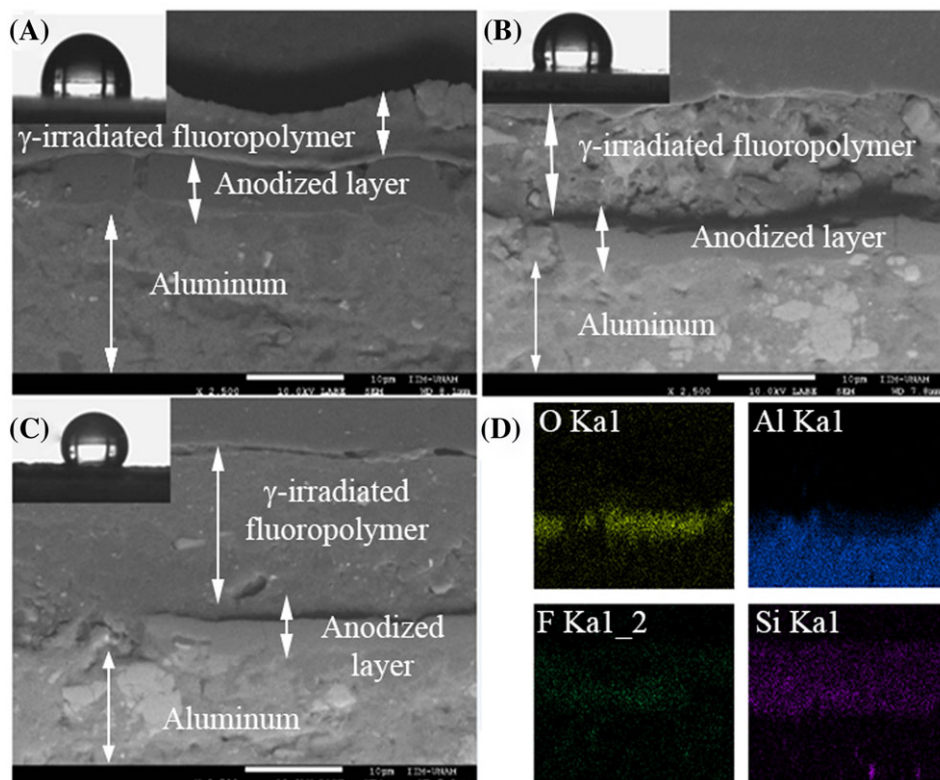

FIGURE 1 Cross-sectional SEM and contact angle images of anodized aluminum with γ-irradiated fluoropolymer sealed with (A) water, (B) dichromate, (C) cerium, and (D) chemical mapping images of cerium sealing

TABLE 1 Electrochemical and physical characteristics of anodized aluminum with γ-irradiated fluoropolymer

Type of sealing	Thickness[a] (μm)	Contact angle	Crystalline structure[b]	R_{corr}[c] (Ω cm^2)	Porosity (%) ×10^{-5}
Water	10.31 ± 0.63	102.3	Amorphous	4.58E + 06	3.05
Dichromate	16.02 ± 0.34	114.7	Amorphous	6.03E + 07	0.36
Cerium	19.61 ± 0.33	128.8	Amorphous	2.56E + 08	0.10

[a]The thickness of the hydrophobic anodized aluminum layer was obtained by SEM.

[b]The crystalline structure was obtained by XRD.

[c]The R_{corr} of the hydrophobic anodized aluminum using a different sealing solution was obtained by EIS.

hand, Figure 1C shows uniform and smooth layers by using the cerium solution. Therefore, the choice of an adequate sealing solution seems to be an important parameter to determine the thickness of the fluoropolymer film above the anodized layer. A thicker and a defect-free fluoropolymer film prevents the absorption of Cl$^-$ ions into the anodized film and into to the oxide/aluminum interface.

Chemical mapping images obtained from the SEM/EDX analyses are included in the results of cerium sealing (Figure 1D) where the presence of the elements for each layer was confirmed. As expected, bare Al was found for the substrate, while O and Al species were detected on the anodized layer because of the electrochemical oxidation of aluminum (Al$_2$O$_3$). Species containing Si and F ions were detected on the γ-irradiated fluoropolymer film because of the chemical chain of the fluorosilane emulsion. The SEM/EDX probe did not detect Ce, but this ion will be later discussed in the XPS analysis.

Table 1 also shows that anodized aluminum with γ-irradiated fluoropolymer had hydrophobic properties with contact angles greater than 100° regardless of the sealing solution. The fluorosilane emulsion

allowed the lowering of the interfacial energy by the replacement of —OH groups by electronegative perfluoro groups.

The X-ray analysis demonstrated that there was no defined crystalline structure on the surface of the hydrophobic/anodized aluminum (Table 1), as has been reported by previous authors.[7,8] The structure has an important influence because amorphous materials exhibit lower surface energy than crystalline lattice which is required to obtain a hydrophobic surface.

The EIS spectra show the corrosion behavior of the sulfuric anodized aluminum (SAA) with the fluoropolymer (FP) layer using different sealing solutions in NaCl. The dielectric properties of the anodized aluminum with the γ-irradiated FP layer are observed in the high-frequency range, while the oxides/hydroxides properties of the metal-anodized layer interface are seen in the low-frequency region (<10 Hz). According to Figure 2A, water boiling sealing had a considerable increase in the impedance values at high and low frequencies compared with pure aluminum; however, the dichromate solution had a better corrosion resistance than boiling water. Finally,
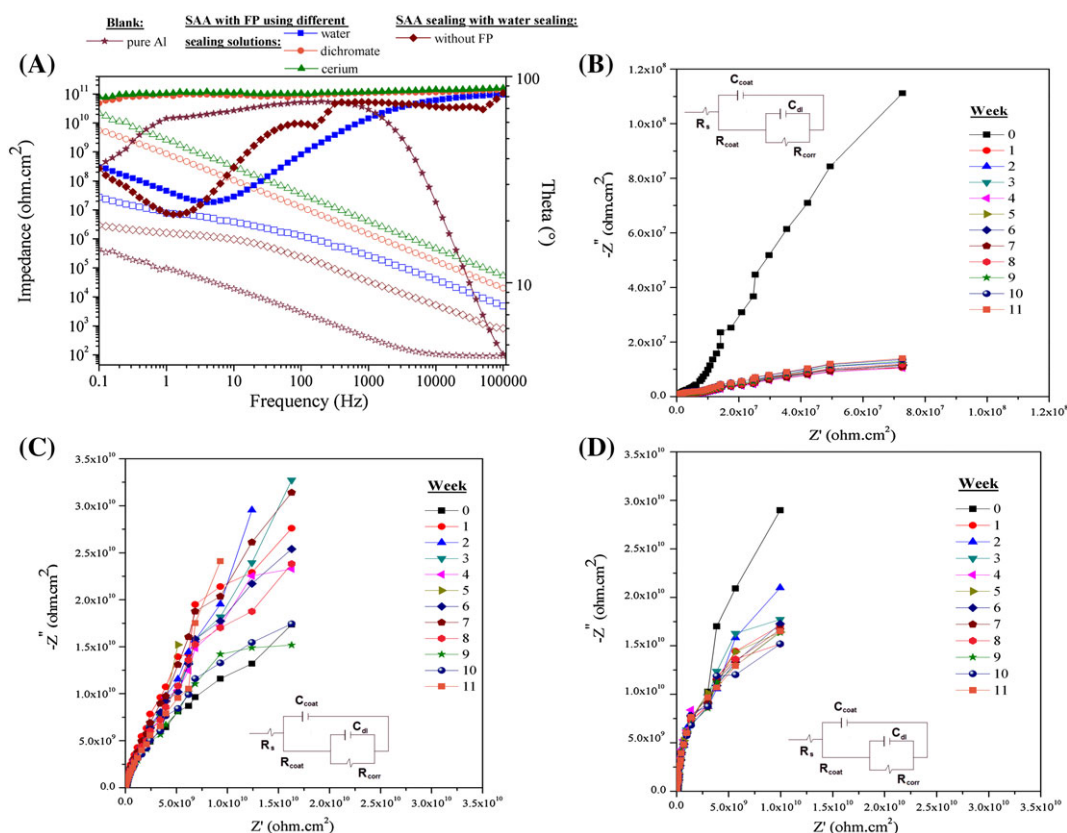

FIGURE 2 EIS diagram of anodized aluminum with γ-irradiated fluoropolymer. (A) Bode plot of sulfuric anodized aluminum (SAA) with and without fluoropolymer (FP); Nyquist diagram of (B) water sealing, (C) dichromate sealing, and (D) cerium sealing during 11 weeks immersed in 0.1 M NaCl
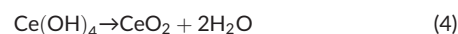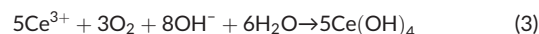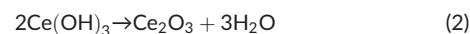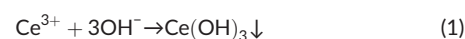
the cerium nitrate sealing performed best with values of 10^5 Ω cm^2 at high frequencies and around 10^{11} Ω cm^2 at low frequencies. In addition to these results, the values of impedance without the incorporation of the γ-irradiated FP above the anodized aluminum layer decreased in comparison with the previous results. This demonstrated the strong affinity between the fluorine silane emulsion and the aluminum oxide to obtaining high impedance values at all frequencies. The Bode plots show the hydrophobic/anodized aluminum testing for 11 weeks of immersion in NaCl (Figure 2B-2D) where the behavior of the cerium sealing displays stable corrosion resistance in time.

An equivalent circuit model is proposed to simulate the EIS results of the hydrophobic/anodized aluminum (inset Nyquist plots). A model of double constant time is applicable for 3 sealing solutions, where R_s represents the solution resistance, R_{coat} and C_{coat} represent the resistance and capacitance of the anodized layer with γ-irradiated FP, while R_{corr} and C_{dl} represent the resistance and the capacitance of the metal/anodized interface, respectively. Based on the thickness measurement obtained by SEM (thickness of hydrophobic/anodized aluminum) in conjunction with the value of R_{corr} obtained by EIS (corrosion resistance of hydrophobic/anodized aluminum using a different sealing solution) and the resistivity of the saline solution (135.5 Ω cm), the degree of porosity was calculated ($\rho_{NaCl}/\rho_{hydrophobic - anodized film}$) x 100 (Table 1). It can be observed that the anodized aluminum sealed with boiling water had the higher quantity of porosity while the anodized aluminum sealed with cerium had the minimum quantity of defects. The cerium sealing reveals the highest values of impedance and largest contact angle which provide a long-term protective layer.

The chemical composition analysis of the anodized aluminum with the γ-irradiated FP layer is shown in Figure 3, where the survey spectra at different depths are shown. The erosion sequence was followed up to 120 minutes; however, the main variations were observed during the first minutes of erosion using the conditions shown in Figure 3.

The presence of the fluorosilane emulsion was detected by the F1s photoelectron and F *KLL* Auger peaks around 687.2 and 832.1 eV, respectively, and the Si peaks at 102.4 (Si 2p) and 153.5 (Si 2s) eV. The intensity of the F peaks increased as the deeper layers were analyzed; meanwhile, the Si signal decreased. Similarly, the O 1s peak at 532.5 eV reduced its intensity with deepness attributable to the replacement of —OH groups by perfluoro groups. In addition, it is important to point out the presence of cerium in Figure 3C (the 3d doublet peaks are clearly observed at 903.4 and 885.0 eV) which confirms the presence of Ce^{4+} used during the sealing process. The intensity of these peaks was higher in the deeper layer. The peak of O is also bonded to Ce because cerium oxide is formed as follows[9]:

$$Ce^{3+} + 3OH^- \rightarrow Ce(OH)_3\downarrow \qquad (1)$$

$$2Ce(OH)_3 \rightarrow Ce_2O_3 + 3H_2O \qquad (2)$$

$$5Ce^{3+} + 3O_2 + 8OH^- + 6H_2O \rightarrow 5Ce(OH)_4 \qquad (3)$$

$$Ce(OH)_4 \rightarrow CeO_2 + 2H_2O \qquad (4)$$

Rare earth ions can form insoluble hydroxides or oxides in NaCl solutions used as cathodic corrosion inhibitors.[10] As described in reaction 1, cerium ions migrate to the bottom of the FP layer where the Ce^{3+} peak is more intense thus enhancing the barrier properties at the interface of anodized aluminum with a γ-irradiated FP. On the other hand, XPS analysis did not detect the dichromate ion, perhaps
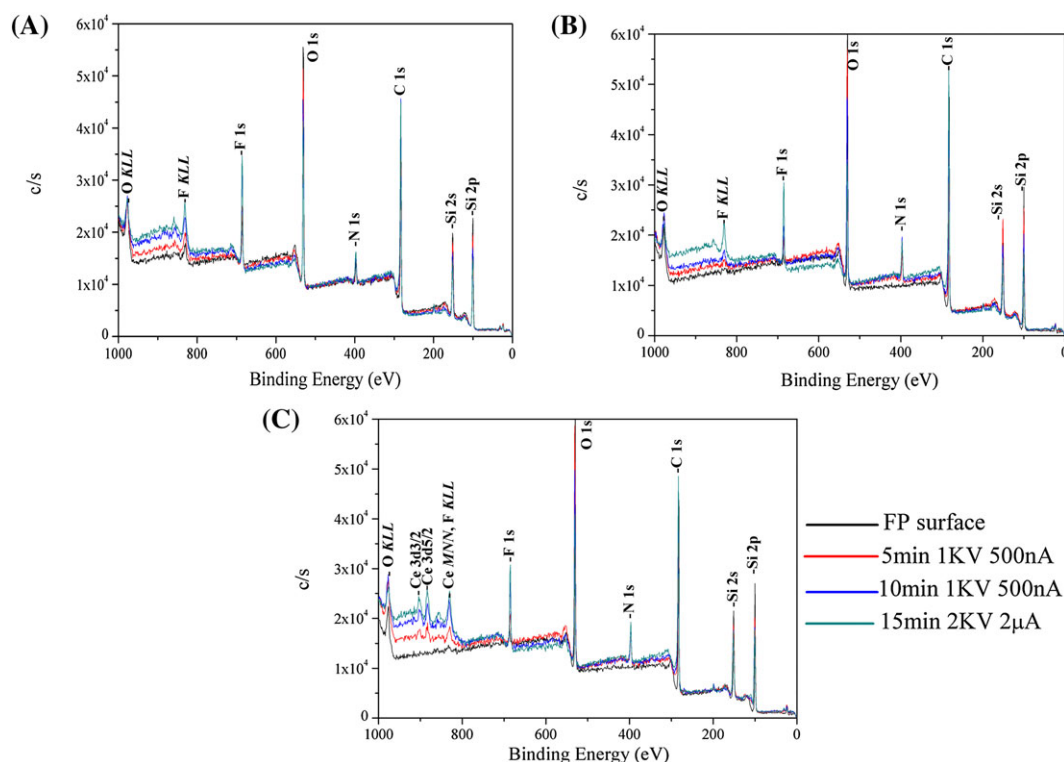

FIGURE 3 XPS spectrum of anodized aluminum with γ-irradiated fluoropolymer (A) water sealing, (B) dichromate sealing, and (C) cerium sealing during 15 minutes of erosion using Ar+ ions
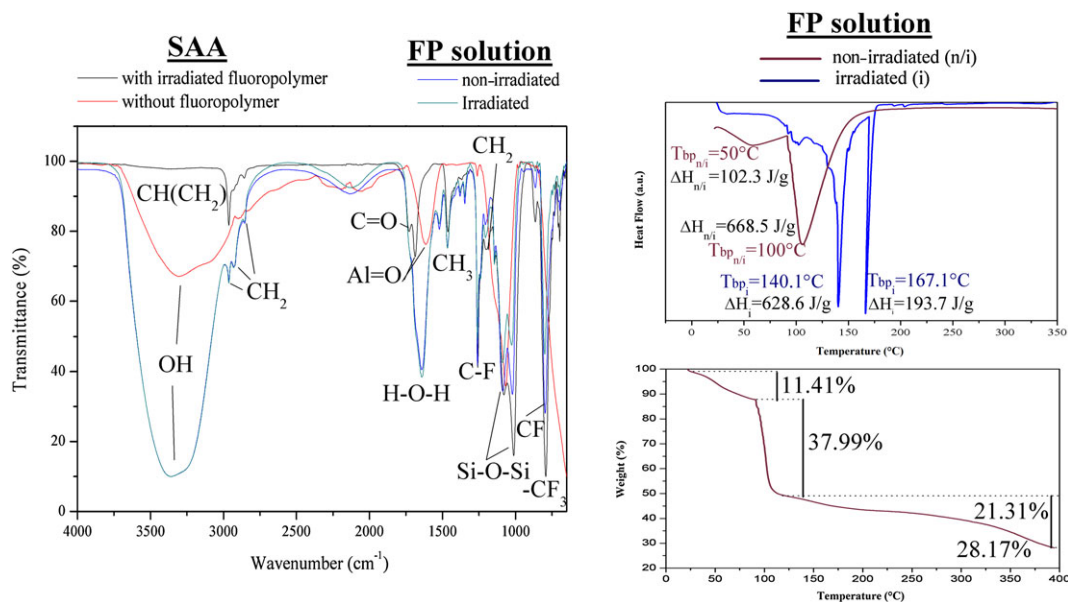
FIGURE 4 Left: IR spectra of sulfuric anodized aluminum (SAA) with/without fluoropolymer (FP) with boiling water sealing and irradiated/no irradiated fluoropolymer emulsion. Right: DSC/TGA curves of irradiated (i) and no irradiated (n/i) fluoropolymer emulsion

because of a deeper migration into the FP layer. However, the effect of dichromate sealing on the corrosion properties is demonstrated in the EIS results.

Concerning the chemical bonds of organic compounds presented in the anodized aluminum with the γ-irradiated FP, an IR spectrum was obtained (Figure 4). Polymers exhibit a characteristic stretching peak at about 2960 cm^{-1} because of CH(CH$_2$) and a stretching vibration of C=O at 1728 to 1731 cm^{-1}. The peak of OH in the stretching mode (3343 cm^{-1}) was identified with SAA without the FP. The interaction between Si—O—Si of the hydrophobic precursor is observed at peaks 1012 to 1080 cm^{-1}. The final reaction of the electrochemical oxidation of aluminum after water sealing Al$_2$O$_3$ + H$_2$O→2AlO(OH) was verified by the presence of AlOOH (boehmite), and this is indicated by Al=O stretching at 1700 to 1500 cm^{-1} for both SAA spectra.

On the other hand, the irradiated and nonirradiated FP solution was also analyzed (same Figure 4). Both spectra are very similar and show the same vibration peaks of organic groups. The broad band at 3400 to 3200 cm^{-1} is related to the polymerization of the FP as O—H stretching vibration and its deformation of H—O—H at 1633 cm^{-1}. Symmetric and asymmetric CH$_2$ as hydrophobic groups were found at 2859, 2927, and 2960 cm^{-1}. The chemical structure of the FPs was confirmed through perfluoroalkyl group vibration where C—F stretching is observed at 1260 cm^{-1} accompanied with a CH$_2$ twisting vibration at 1191 cm^{-1}. The low surface energy group, —CF$_3$, was found near to 890 cm^{-1} accompanied with CF deformation vibration.

Concerning the DSC results, Figure 4 (right) shows the different DSC/TGA thermograms of the irradiated and nonirradiated FP solutions. Before γ-irradiation, 2 endothermic peaks can be observed at 50°C with ΔH = 102.3 J g^{-1} and 100°C with 668.5 J g^{-1}. These 2 peaks are related to the boiling points of volatile compounds. TGA demonstrated a loss mass of 11.41% and 37.99% at each peak; thus, after the second peak, a loss mass of 50% was evidenced. After 110°C, the loss mass was gradually decreased; this indicates the slow

decomposition of the nonvolatile part of the FP. At 400°C, 72% of mass was decomposed. A similar TGA thermogram was obtained for the irradiated fluoropolymer. After this irradiation process, the 2 peaks moved to 140.1°C with ΔH = 628.6 J g^{-1} and 167.1°C with ΔH = 193.7 J g^{-1} revealing that these temperature displacements with their respective changes in enthalpy shows stronger perfluoroalkyl bonds[4,11] which induce higher corrosion resistance. After 200°C, no thermal transition was observed which means a continuous decomposition.

4 | CONCLUSION

The γ-irradiated FP notably improved the corrosion properties of the sulfuric anodized aluminum. Different sealing solutions were used to enhance the corrosion resistance. It was demonstrated that boiling water, dichromate, and cerium sealings affected the thickness of the fluoropolymer and the morphology of the hydrophobic/anodized aluminum. The cerium species, mostly detected throughout the anodized layer/fluoropolymer interface, exhibited the highest values of impedance resistance at all frequencies with the largest contact angle values. The amorphous structure of the anodized aluminum with the γ-irradiated fluoropolymer favors hydrophobicity properties thus improving barrier properties at the interface metal-anodized layer.

ORCID

R. Jaimes-Ramírez http://orcid.org/0000-0002-8681-1706

A. Covelo http://orcid.org/0000-0003-3053-9624

M. Hernández http://orcid.org/0000-0003-3153-8359

REFERENCES

1. Heakal F, Shehata O, Awad A. Relevant aspects in the stability performance of different anodic alumina (AAO) films in aqueous sulfate solutions. *J Electroanal Chem*. 2017;792:95-103.

2. Whelan M, Barton K, Cassidy J, Colreavy J, Duffy B. Corrosion inhibitors for anodised aluminium. *Surf Coat Technol*. 2013;227:75-83.

3. Ramírez HB. *Estudio y caracterización del anodizado en aleaciones de aluminio AA2024-T3 para la incorporación de recubrimientos de sol-gel*. México: Tesis de Licenciatura, Universidad Nacional Autónoma de México; 2014:142.

4. Gueven O. An overview of current developments in applied radiation chemistry of polymers. In: *Proceedings of a Technical Meeting. Adv Radiat Chem Polym*. Indiana, USA: IAEA; 2004:33-39.

5. Hao L, Cheng BR. Sealing processes of anodic coatings—past, present and future. *Met Finish*. 2000;98(12):8-18.

6. Wang S, Zhao Q, Du N, Shao Z, Shu W, Chen Q. Sealing effect of cerium salt on boric-sulfuric acid anodic film of aluminum alloy. *Chin J Nonferrous Met*. 2012;22:1132-1141.

7. Mohammadi I, Afshar A, Ahmadi S. Al$_2$O$_3$/Si$_3$N$_4$ nanocomposite coating on aluminum alloy by the anodizing route: Fabrication, characterization, mechanical properties and electrochemical behavior. *Ceram Int*. 2016;42(10):12105-12114.

8. Roshani M, Sabour Rouhaghdam A, Aliofkhazraei M, Heydari Astaraee A. Optimization of mechanical properties for pulsed anodizing of aluminum. *Surf Coat Technol*. 2017;310:17-24.

9. Lakshmi RV, Aruna ST, Anandan C, Bera P, Sampath S. EIS and XPS studies on the self-healing properties of Ce-modified silica-alumina hybrid coatings: Evidence for Ce(III) migration. *Surf Coat Technol*. 2017;309:363-370.

10. Hamdy AS, Beccaria A. Effect of surface preparation prior to cerium pre-treatment on the corrosion protection performance of aluminum composites. *J Appl Electrochem*. 2005;35(5):473-478.

11. Czvikovszky T. Radiation-assisted compatibilization of polymers. In: *Proceedings of a Technical Meeting. Adv Radiat Chem Polym*. Indiana, USA: IAEA; 2004:61-74.